

Towards User Scheduling for 6G: A Fairness-Oriented Scheduler Using Multi-Agent Reinforcement Learning

Mingqi Yuan¹, Qi Cao, Man-On Pun, *Senior Member IEEE* and Yi Chen

Abstract—User scheduling is a classical problem and key technology in wireless communication, which will still play an important role in the prospective 6G. There are many sophisticated schedulers that are widely deployed in the base stations, such as *Proportional Fairness* (PF) and *Round-Robin Fashion* (RRF). It is known that the *Opportunistic* (OP) scheduling is the optimal scheduler for maximizing the average user data rate (AUDR) considering the *full buffer* traffic. But the optimal strategy achieving the highest fairness still remains largely unknown both in the full buffer traffic and the *bursty* traffic. In this work, we investigate the problem of fairness-oriented user scheduling, especially for the RBG allocation. We build a user scheduler using *Multi-Agent Reinforcement Learning* (MARL), which conducts distributional optimization to maximize the fairness of the communication system. The agents take the cross-layer information (e.g. RSRP, Buffer size) as *state* and the RBG allocation result as *action*, then explore the optimal solution following a well-defined *reward* function designed for maximizing fairness. Furthermore, we take the *5%-tile user data rate* (5TUDR) as the key performance indicator (KPI) of fairness, and compare the performance of MARL scheduling with PF scheduling and RRF scheduling by conducting extensive simulations. And the simulation results show that the proposed MARL scheduling outperforms the traditional schedulers.

Index Terms—User scheduling, RBG allocation, Fairness-oriented, Multi-Agent reinforcement learning

I. INTRODUCTION

FOR the prospective 6G wireless communication technology, both of the basic architectures and components remain largely undefined [1]. It is foreseeable that the 6G will bring an unprecedented revolution while meeting the tremendous and increasing network demand. The utilization of 5G greatly improves the communication services in densely populated cities, especially for the indoor communication scenarios. However, there are still a large number of population can not obtain the basic data services, such as the developing countries and rural areas [2]. The 6G is predicted to be human centric, data centric rather than machine centric [3]. So the

6G is expected to construct a wireless network which is both vertical and horizontal to benefit more population rather than the majority people in cities. This expectation emphasizes the fairness of the network resources scheduling, which is difficult to optimize in the previous studies.

In this paper, we investigate the problem of the user scheduling, especially the Resource Block Groups (RBGs) allocation. But we consider the fairness-oriented scheduling and aim to build a scheduler which maximizes the fairness of the network. As the Key Performance Indicators (KPI), the average user data rate (AUDR) and fairness are usually adopted to evaluate the schedulers. It is known that the Opportunistic (OP) scheduling is the optimal scheduler which maximizes the AUDR considering the full buffer traffic [4]. The OP scheduling follows the greedy policy and always allocates advantageous resources to the users with the highest expected transmission rate. However, the optimal strategy achieving the highest fairness has not been studied both in the full buffer traffic and the bursty traffic. Furthermore, the definition and the measurement of the fairness are still debatable until today. Consider the allocation time, the Round Robin Fashion (RRF) is regarded as the optimal scheduler in the full buffer traffic [5]. The RRF scheduling allocates all the resources to each user in turns regardless of their status. This scheduler indeed realizes the allocation time equality but it may waste much network resources. Because a user will get all the resources even its data packets is exhausted. In this era with tremendous network demands, the time-fairness is apparently obsolete and the rate-fairness is proposed. Therefore the 5%-tile user data rate (5TUDR) is more widely leveraged to evaluate the fairness of the network [6], which is the user data rate of the worst 5% user. Compared with the time-fairness, the 5TUDR emphasizes the right of the inferior users but it does not go against the AUDR. So it is likely feasible to maximize the 5TUDR while maintaining the considerable AUDR.

There are two main challenges in realizing the objective. On the one hand, the wireless communication network is highly complex with multi components and mechanism, rendering the task of mathematically modeling the whole system analytically intractable. Most of the traditional model-based schedulers are designed on single layer of the OSI protocol, which can only take poor information to make allocation. For instance, the Proportional Fairness (PF) scheduling calculates the allocation priorities by tracing the user data rate recorded by the MAC layer [7]. But the network performance is affected by multi

This work was supported, in part, by the Shenzhen Science and Technology Innovation Committee under Grant No. ZDSYS20170725140921348 and JCYJ20190813170803617, and by the National Natural Science Foundation of China under Grant No. 61731018. (*Corresponding author: Man-On Pun.*)

M. Yuan, Q. Cao, M. Pun and Y. Chen are with the School of Science and Engineering, The Chinese University of Hong Kong, Shenzhen, 518172, China (e-mail: mingqiyuan@link.cuhk.edu.cn; caoqi@cuhk.edu.cn; simonpun@cuhk.edu.cn; yichen@cuhk.edu.cn.)

M. Yuan, Q. Cao and M. Pun are with the Shenzhen Key Laboratory of IoT Intelligent Systems and Wireless Network Technology, 518172, China

M. Yuan, M. Pun and Y. Chen are with the Shenzhen Research Institute of Big Data, 518172, China

layers, thus it is difficult to achieve higher fairness through the model-based approaches. On the other hand, studying the bursty traffic is considered as a non-stationary task, it brings unaccountable uncertainty such as the time-varying number of the users. Moreover, the 5TUDR is affected by the long-term allocation steps, it is difficult to optimize such objective only by optimizing single-step allocation.

To address the dilemma, the machine learning (ML) methods are introduced to the research of wireless communication [8] in recent years. In sharp comparison with the model-based approach, the ML-based method is data-driven which applies optimization by exploiting the massive data in the network. This allows the ML-based method to solve many network optimization problems without establishing the mathematical model. For instance, Cao et al. designed a DNN-based framework to predict network-level system performance which take the cross-layer network data as input [9]. And the simulation results show that the model can make accurate predictions at the cost of high computational complexity. For user scheduling, another method entitled Reinforcement Learning (RL) is also introduced to improve the existed schedulers or build new schedulers. RL is one of the most representative leanings methods of machine learning, which aims to maximize the long-term expected return by learning from the interactions with environment [10]. In RL, the agent accepts the state of environment and make corresponding action, then the agent will be rewarded or punished. To get higher reward, the agent must continuously adjust its policy to make better action. The RL has strong exploration ability, and always achieve surprising performance. There are much pioneering work have already been achieved with RL.

For instance, Comsa et al. suggests that the PF scheduling cannot adapt to dynamic network conditions because of the settled scheduling preference [11]. Thus they proposes a parameterized PF scheduling entitled Generalized PF (GPF) by using the deep RL approach. The GPF collects diverse network data such as Channel Condition Indicator (CQI) and user throughput, then adaptively adjust the scheduling preference in each transmission time interval (TTI). As a result, the GPF is showed to be more flexible in handling dynamic network conditions. Furthermore, Zhang et al. builds an RL-enabled algorithm selector, which scans the network status and intelligently select the best scheduling algorithm from a set of scheduling algorithms in each TTI [12]. And the simulation results show that the fusion strategy achieves higher performance compared to the traditional methods. However, both of the two algorithms have low efficiency because of the huge computation, and they are not independent schedulers. Therefore, Xu et al. considers building entirely independent schedulers with RL method [13], and proposes an RL-based scheduler. The scheduler takes the estimated instantaneous data rate, the averaged data rate and other metrics as the input of the agent, then outputs the allocation preference for each user. The performance comparison in [13] indicates that the RL-based scheduler can effectively improve the throughput, along with the fairness and the packet drop rate. But this

scheduler can only allocate RBGs in full buffer traffic, because it takes fully-connected neural network as the backbone of agent. Similarly, Hua et al. investigates the resource management in network slicing, and proposes a GAN-powered deep distributional RL method to find optimal solution of demand-aware resource management [14]. The agent takes the number of arrived packets in each slice within a specific time window as input, then generates bandwidth allocation to each slice. And the simulations results show that method significantly improve the utilization efficiency of resources.

In this work, we consider a Long-Term Evolution (LTE) network with one base station (BS) scheduling its RBGs to multiple users in the bursty traffic. Take the allocation result of RBGs as the action in RL, the multi RBGs produce a joint action. For single agent RL, it is difficult to learn a joint policy because of the exponential action space. Thus we leverage the Multi-Agent Reinforcement Learning (MARL) to address the problem, which maintains multi agents and learns a distributional policy [15]. As there are multi agents interacting with the environment, this can be regarded as a game from the perspective of the game theory, which takes the Nash Equilibrium (NE) as the optimal solution [16]. Inspired by the distributional setting and powerful exploration abilities of RL, the MARL offers a solution paradigm that can cope with complex problems. One of the most successful applications is AlphaStar, which is a game AI for the StarCraft II using MARL [17]. The AlphaStar can achieve grandmaster level performance in the confrontation with mankind, which implies the great potential of MARL.

In this work, we first model the RBG allocation process as a stochastic game, in which each RBG is allocated by a specific agent independently. All the agents are set to be fully cooperative, which share the same reward function and maximize the objective together. Then a MARL algorithm entitled QMIX is leveraged to find the scheduling policy. Finally, we compare the performance of the MARL scheduler with the PF scheduling and RRF scheduling. The simulation results show our method outperforms the two traditional model-based algorithms. The main contributions of this paper are as follows:

- We analyze the necessity of fairness-oriented scheduling algorithm in the development of 6G, which is expected to provide more equitable network service. Then the main challenges of building such algorithms are fully discussed, and we summarize the applications of data-driven approaches in wireless communication, especially the wireless resource management;
- To build the fairness-oriented scheduling policy, we first build a LTE downlink wireless network to simulate the realistic communication scenarios. Then we model the RBG allocation process as a stochastic game, and skillfully define its components such as state, action and reward function. Moreover, we build the stochastic game considering the bursty traffic, which brings dynamic network conditions such as the time-varying number of active users. A adaptive working mechanism of the agents

is proposed;

- The reward function characterizes the optimization objective of the agents, which is difficult to be obtained and always experience-based. To find the feasible reward function that maximizes the 5TUDR, we dive into the design of the reward function and develop a fairness-oriented reward function, which is shown to be effective in realizing our objective;
- Based on the proposed stochastic game, we build a MARL-based algorithm to search the expected scheduling policy. The workflow of this algorithm is carefully summarized. With a large number of training, the expected scheduling policy is successfully obtained, it achieves high 5TUDR while maintaining a considerable AUDR.
- Finally, extensive simulations are conducted to demonstrate the better performance of the MARL scheduler over the traditional schedulers. Furthermore, we analyze the special scheduling policy of the MARL scheduler in depth by data analysis, and provide numerical results about the implementation details.

The remainder of the paper is organized as follows: Section II defines the system model and gives the problem formulation. Section III elaborates the framework of the stochastic game for RBG allocation. Then Section IV introduces the MARL algorithm for solving the stochastic game. And Section V shows the simulation results and numerical analysis. Finally, Section VI summarizes the paper and proposes the prospects.

II. SYSTEM MODEL AND PROBLEM FORMULATION

A. System Model

We consider a single-cell LTE wireless communication network in which a BS serves multiple user equipments (UEs) in the downlink in the Frequency Division Duplexing (FDD) mode. The UE arrival is modeled as following a distribution, such as the Poisson distribution with an arrival rate λ . Upon arrival, each UE requests a different but finite amount of traffic data that is stored in the buffer at the transmitter. After its request is completed, the corresponding UE departs the network immediately, which effectively simulates the bursty traffic mode. Furthermore, the frequency resources are divided into RBGs. We consider the most common network setting that one RBG can be allocated to at most one UE in each TTI as shown in Fig. 1. There are k RBGs and four users in the network. At each TTI, if a user is scheduled, the corresponding data will be loaded to a HARQ buffer and cleared out from the data buffer. For each user, it can only maintain finite HARQ processes, and the ACK/NACK message will be fed back with fixed time period. The more specific network mechanisms such as retransmission and OLLA process are elaborated in Appendix A. Based on the network, we aim to build an RBG allocation algorithm to realize intelligent and flexible scheduling, so as to maximize the 5TUDR in the bursty traffic while maintaining considerable AUDR.

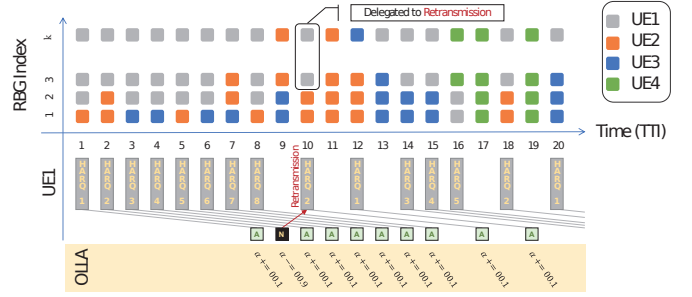


Fig. 1. Network Mechanisms

B. Problem Formulation

To formulate the specific optimization problem, we first define two key performance indicators for evaluating the utility of the schedulers. One is the average user data rate (AUDR) which measures the usage of the network resources. The other one is the 5%-tile user data rate (5TUDR) which assesses the fairness of the scheduling.

1) *Key Performance Indicators*: Denote by $t_{n,a}$ and $t_{n,d}$ the arrival and departure time for a user indexed by n , respectively. The user data rate (UDR) of user n at time $t \in [t_{n,a}, t_{n,d}]$ can be defined as:

$$\psi_t^n = \frac{\sum_{i=t_{n,a}}^t T_n[i] \mathfrak{A}_n[i]}{\min(t, t_{n,d}) - t_{n,a}}, \quad (1)$$

where $T_n[i]$ is the packet size transmitted during the i -th TTI, and $\mathfrak{A}_n[i]$ is the ACK/NACK feedback with "1" indicating a successful transmission while "0" a failed transmission. Denote by N_t the total number of users that arrive during a time period of $\text{TTI}=[1, \dots, t]$. The AUDR can be defined as

$$D(t) = \frac{1}{N_t} \sum_{n=1}^{N_t} \psi_t^n. \quad (2)$$

Finally, let ϕ_t denote the 5%-tile user data rate, which can be written as:

$$\phi_t = \mathfrak{T}(\Psi_t), \Psi_t = (\psi_t^1, \dots, \psi_t^{N_t}) \quad (3)$$

where $\mathfrak{T}(\cdot)$ is the searching operator for getting the user data rate of the worst 5% user.

2) *Optimization Objective*: In this paper, we aim to maximize the 5TUDR in the bursty traffic, while maintaining a considerable AUDR. Given a network defined above with a set K of RBGs, we set the maximum number of users as M in each TTI. We choose to optimize the 5TUDR in a finite time horizon, where the arrival of the users follows a specific distribution. Take the Poisson distribution for instance, we set the arrival rate of the users as λ . Denote by π the scheduling policy. For a period $\text{TTI}=[1, \dots, T]$, the optimization problem is written as:

$$\max_{\pi} \phi_T \quad (4)$$

subject to

$$\begin{aligned} \psi_t^n &\geq 0, 1 \leq t \leq T, 1 \leq n \leq N_t \\ D(T) &\geq \kappa \\ P(N_T) &= \frac{\lambda^{N_T}}{N_T!} e^{-\lambda} \end{aligned}$$

where the $P(\cdot)$ being the probability, κ is the threshold.

However, it is mathematically intractable to find such a policy π via traditional optimization methods because of the highly complex network components and mechanisms. In the following sections, we transform this scheduling problem into a stochastic game where the RBGs are allocated by multi agents. Moreover, the cross-layer network data is leveraged to serve as the observations in the game, so as to make allocation from the global perspective. Finally, a MARL-based algorithm is proposed to search the solutions.

III. STOCHASTIC GAME FRAMEWORK FOR RBG ALLOCATION

There are two main challenges when solving the Op. 4 in the bursty traffic. On the one hand, the actual user data rate is affected by multiple factors of different layers, it is almost impossible to build mathematical model and solve it through traditional optimization methods. The 5TUDR is a special variable which is affected by the sequence of the allocation steps. Straightforwardly optimizing single-step scheduling may not contribute to this item, where the long-term optimization is indispensable. On the other hand, allocating multi RBGs to multi users can be considered as conducting a joint action, which produces exponential action space. Searching solution in this action space is always intractable both in solvability and computation.

To address the two main challenges, we consider optimizing the objective via long-term and distributional method. A traditional model-based scheduler allocates all the RBGs following the same scheduling policy. This allows the scheduler to stably optimize a fixed objective, e.g., system throughput or fairness. But a static policy is short of flexibility and adaptability, which can not cope with complex network conditions. In sharp contrast to the centralized policy, the distributional policy decomposes the exponential action space into smaller individual action space, and optimize the objective more efficiently. Based on the distributional policy, we further leverage the cross-layer network data to make allocation. The traditional model-based scheduler always take the single-layer network data as decision basis, e.g., the PF scheduling takes the user data rate to calculate the allocation priorities. But cross-layer network data contains more comprehensive decision information, which may contribute to the scheduling from a wider perspective.

To learn such a distributional scheduling policy, we first model the RBG allocation process as a stochastic game, which is the generalization of the Markov Decision Process (MDP) for the multi-agent cases.

Definition 1. *This stochastic game can be defined by a tuple $\mathcal{E} = \langle \mathcal{S}, \mathcal{U}, \mathcal{A}, \mathcal{P}, r, \mathcal{Z}, \mathcal{O}, \gamma \rangle$ [18], where:*

- \mathcal{S} is the global state space;
- \mathcal{U} is the action space for each agent;
- \mathcal{A} is a set of agents and each agent is identified by $a \in \mathcal{A}$;
- $\mathcal{P}(s'|s, \mathbf{u})$: $\mathcal{S} \times \mathcal{U} \times \mathcal{S} \rightarrow [0, 1]$ is the transition probability, where $\mathbf{u} \in \mathcal{U} \equiv \mathcal{U}^{|\mathcal{A}|}$;
- $r(s, \mathbf{u}, a)$: $\mathcal{S} \times \mathcal{U} \times \mathcal{A} \rightarrow \mathbb{R}$, the reward function which specifies an agent its specific reward;
- \mathcal{Z} : agents draw its individual observation $z \in \mathcal{Z}$;
- $\mathcal{O}(s, a)$: $\mathcal{S} \times \mathcal{A} \rightarrow \mathcal{Z}$ is the observation function;
- $\gamma \in [0, 1]$ is a discount factor.

We further consider the partially observable settings, in which agents get local observations o_a^t based on observation function $\mathcal{O}(s, a)$ [19] [20]. Thus each agent has an action-observation history $\tau^a \in \mathcal{T} \equiv (\mathcal{Z} \times \mathcal{U})^*$, which is conditioned by a stochastic policy $\pi^a(u^a|\tau^a)$: $\mathcal{T} \times \mathcal{U} \rightarrow [0, 1]$. All the local policies constitutes the joint-policy π , and the distribution over the joint-action can be formulated as:

$$\pi(\mathbf{u}|s_t) = \prod_a \pi^a(u^a|\tau^a) \quad (5)$$

The Fig. 2 illustrates the overview of this stochastic game. The base station holds a set of K RBGs and accepts the UEs, then follows the scheduling policy π to allocate RBGs. In this game, $|K|$ agents are built to allocate the RBGs respectively. Each agent maintains an independent scheduling policy which is only responsible for its own RBG. At each TTI, the agents observe the network data of the cell, which constitutes the state s . The scheduling policy π accepts the state and makes corresponding action \mathbf{u} . Here the action is the allocation result, it determines each RBG should be allocated to which user. Then the base station accepts the allocation result and conduct transmission as required. Finally, the environment will evaluate the state-action pair and calculate a reward. As for the policy update procedure, it will be elaborated in section IV. In the following subsections, the specific forms of states, actions and reward function in the stochastic game of RBG allocation are elaborated in detail.

A. Cross-layer Observation and Adaptive Action

Initialize a base station with a set of K RBGs, and randomly generate \hat{N} active users. For a traditional model-based scheduler, it only observes the single-layer information of the network, such as MAC layer or PHY layer. The limitation of the mathematical models makes the allocation lack the support comprehensive information. To address the problem, we consider conduct the scheduling based on cross-layer information. To handle the cross-layer network data, the deep neural network (DNN) is leveraged to serve as the backbone of the agents. Hornik et al. has proved that standard multilayer feedforward networks are capable of approximating any measurable function to any desired degree of accuracy [21]. The DNN can provide powerful feature extraction ability and approximate arbitrary functions [22]. This allows us to straightforwardly take the cross-layer network data as the

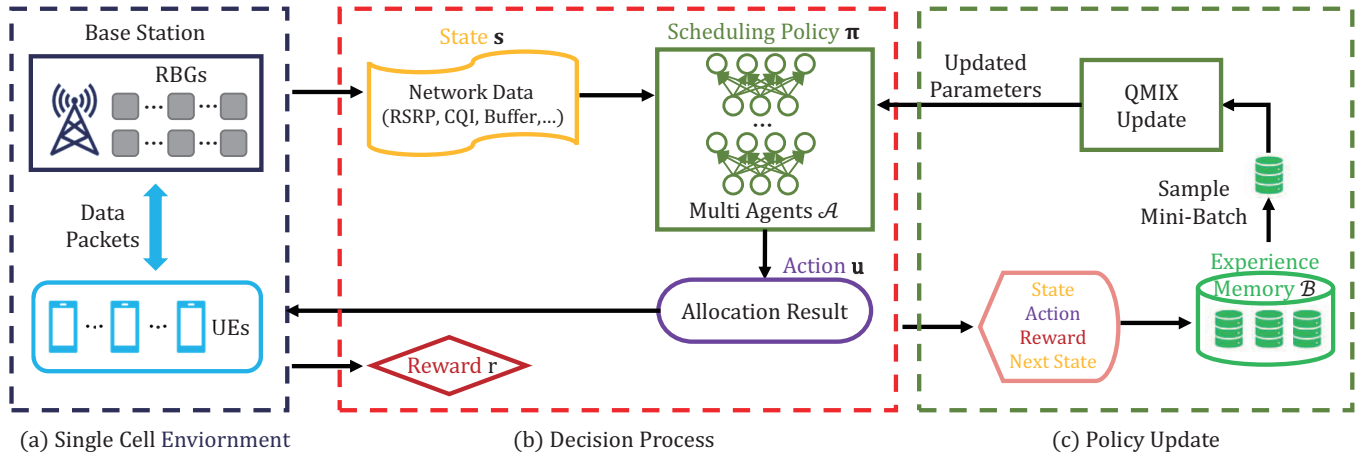


Fig. 2. The overview of the stochastic game of the RBG allocation. (a) A single cell which contains a base station and UEs. (b) The decision process of the scheduling policy π . (c) The update procedure of the scheduling policy, where the QMIX is a MARL learning algorithm introduced in section IV.

observation, then make actions according to the output of the DNN.

TABLE I
NETWORK DATA OF GLOBAL STATE

| Attr. | Layer | Dim. |
|----------------------------------|-------|--------------|
| RSRP | PHY | 1 |
| Average of RB CQI (each RBG) | PHY | Num. of RBGs |
| Buffer size | MAC | 1 |
| Scheduled times | MAC | 1 |
| Olla offset | MAC | 1 |
| Historical user data rate (HUSR) | MAC | 1 |

Table I illustrates the selected network data in this paper. Reference Signal Receiving Power (RSRP) is one of the key parameters that can represent the wireless signal strength in LTE networks. This metric is a constant through the interaction between user and base station, which can straightforwardly reflects the level of the final transmission rate. Channel Quality Indicator (CQI) is the information indicator of channel quality, which represents the current channel quality and corresponds to the signal-to-noise ratio (SNR) of the channel. For each user, it has different CQI on different RBGs. This metric is adopted referring to the OP scheduling. To maximize the throughput, the OP scheduling prefers to allocate more RBGs to advantageous users who take higher expected transmission rate. Here the buffer size is the data packets need to be transferred. It affects the residence time of the users in the bursty traffic. Here the schedule times is designed for representing the probability fairness, which indicates whether all the users have same probability to get the RBGs. Finally, the HUSR is collected referring to the PF scheduling. The PF scheduling calculates the allocation priorities for each user by tracing the HUSR and instantaneous UDR. And the configured agents are expected to take such metrics into consideration when conducting the allocation.

Denote by $F = \{\mathbf{f}^1, \dots, \mathbf{f}^{|F|}\}$ the set of selected network

data from different layers, then the global state can be formulated as a feature matrix:

$$\mathbf{S} = (\mathbf{f}^1, \dots, \mathbf{f}^{|F|}), \mathbf{f}^i = (f_1^i, \dots, f_N^i)^T \quad (6)$$

For the *bursty traffic*, the feature matrix is a variable due to the time-varying number of the active users in the cell. It also means the agents need to allocate fixed RBGs to an uncertain number of users. However, the fully-connected neural networks (FCNN) only accepts input with fixed dimensions along with the output [23]. To address this problem, the projection operation is applied to the state matrix \mathbf{S} :

$$\mathbf{s} = \mathfrak{F}(\mathbf{S}^T \mathbf{S}), \mathbf{s} \in \mathbb{R}^{|F|^2} \quad (7)$$

where $\mathfrak{F}(\cdot)$ is a flattening operator, it flattens a matrix into a vector by row and generates a vector with fixed dimensions. Because many selected attributes are continuous values, which is almost impossible to generate absolutely same \mathbf{s} .

TABLE II
NETWORK DATA OF LOCAL OBSERVATIONS

| Attr. | Layer | Dim. |
|----------------------------------|-------|------|
| RSRP | PHY | 1 |
| Average of RB CQI | PHY | 1 |
| Buffer size | MAC | 1 |
| Scheduled times | MAC | 1 |
| Olla offset | MAC | 1 |
| Historical user data rate (HUSR) | MAC | 1 |

Based on the global state, we design the local observations using the subset of F (listed in Table II), which can be written as:

$$\mathbf{O} = (\mathbf{f}^1, \dots, \mathbf{f}^{|\hat{F}|}), \mathbf{f}^i = (f_1^i, \dots, f_N^i)^T, \hat{F} \subset F \quad (8)$$

As can be seen in Table II, the agents share some public network data such as the buffer size and the HUSR, while

keeping its unique attributes. Since each RBG is allocated by a agent independently, it only needs to observe its own CQI on the UEs. Moreover, this exclusive feature highlights the uniqueness of each RBG, which may motivates the agents to explore diverse scheduling polices.

Similarly, the projection operation is also applied to the local observations to generate a fixed vector:

$$\mathbf{o} = \mathfrak{F}(\mathbf{O}^T \mathbf{O}), \mathbf{o} \in \mathbb{R}^{|\hat{F}|^2} \quad (9)$$

As the DNN is leveraged to be the backbone of the agents, we let $\pi_{\theta_a}^a$ denote the policy of agent a , which is parameterized by a fully-connected network with parameters θ_a . For RBG allocation, the policy accepts a local observation \mathbf{o}^a and generates \hat{N} priorities for \hat{N} users, then the RBG is allocated to the user with the highest priority:

$$u_a = \arg \max_{u_a} \{\pi_{\theta_a}^a(\mathbf{o}^a)\} \quad (10)$$

All the local actions constitute the joint-action \mathbf{u} , which can be written as follows when there are $|K|$ RBGs and \hat{N} active users in the cell:

$$\mathbf{u} = (u^1 \dots u^{|K|}), u^a \in \{1, \dots, \hat{N}\} \quad (11)$$

Similar to time-varying problem in the definition of observation, the policy also needs to make adaptive allocation due to the time-varying \hat{N} . However, limited by the properties of the FCNN, it can not generate adaptive output.

As there is a maximum user capacity M , then the users in the cell can be divided into two parts: \hat{N} active users and $M - \hat{N}$ virtual users. Then we set the output layer of the policy network with M neurons to generate M priorities. Finally, select the action using the former \hat{N} values. The Fig. 3 illustrates the operation.

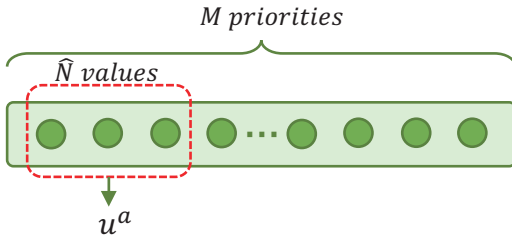


Fig. 3. Adaptive action

Moreover, all the network data of the virtual users will be set as 0, and this will not affect the final values of the observation vector due to the properties of the projection. With a lot of interactions and training, the agents are feasible to learn the corresponding pattern.

B. Fully Cooperative Game

As the final user data rate is determined by the usage of all resources, so we set all the agents are fully cooperative in this game, this implies that all the agents receive the same reward and make it as a global reward [16]:

$$r(\mathbf{s}, \mathbf{u}, a) = r(\mathbf{s}, \mathbf{u}, a'), \forall a, a'. \quad (12)$$

As the agents are set to be fully cooperative, the reward function is rewritten as $r(\mathbf{s}, \mathbf{u})$ for convenience in the following sections.

In this paper, we aims to maximize the 5TUDR in the bursty traffic. Since the reward function characterizes the optimization objective of the game, it should outputs the gain performance to the final 5TUDR of each state-action pair. Considering a time period $\text{TTI}=[1, \dots, T]$, this reward function evaluates the contribution of each allocation step to the final 5TUDR.

Thus the optimization objective in the Op. 4 is transformed into:

$$\max_{\pi} \mathbb{E} \left[\sum_{t=1}^T \gamma^t r_t(\mathbf{s}_t, \mathbf{u}_t) | \pi \right] \quad (13)$$

s.t.

$$\begin{aligned} \psi_t^n &\geq 0, 1 \leq t \leq T, 1 \leq n \leq N_t \\ D(T) &\geq \kappa \\ P(N_T) &= \frac{\lambda^{N_T}}{N_T!} e^{-\lambda} \end{aligned}$$

where π being the joint policy.

The Eq. 13 indicates that the objective of this stochastic game is to find a joint-policy π which maximizes the long-term return. And the agents are allowed to explore diverse polices as long as the Eq. 13 is maximized. However, the design of the reward function lacks rigor theoretical support in practice, most of the configurations are always experience-based. In next section, we dive into the design of the reward function, and discuss the taken insights from comprehensive perspective.

C. Reward Function

The RRF scheduling achieves the highest time-fairness because each user can get the responses equally. But this scheduling policy does not take account of the usages, which wastes much available network resources. So we argue that the promotion of the 5TUDR should not largely decrease the average user data rate. Considering the network capacity, we hope to maximize the 5TUDR while maintaining considerable AUDR.

Intuitively, to maximize the 5TUDR, it is natural to take the increment of 5TUDR as the reward function. But this reward function is founded to be incompatible with the bursty traffic. To demonstrate the conflict, we trace the variation of 5TUDR in one random communication process which lasts 500TTIs. As can be seen in the Fig. 4, the increment of 5TUDR is always 0, and there are some sharp increase and sharp decrease in the figure. The sharp decrease is because of the arrival of new users, if a new user arrives at the base station at TTI t , the ϕ_t will suddenly become 0 because the new user has no transmitted data packets. Once the new user is scheduled, its user data rate will soar, which causes the sharp increase.

Therefore, this reward function can not cope with the bursty traffic and properly evaluates the actions.

Similarly, we can take the increment of AUDR as the reward function, which aims to improve the 5TUDR via improving the AUDR. But this will also be affected by the time-varying number of the active users. Fig. 5 illustrates the increment of AUDR between two adjacent TTI in one simulation. There are also some sharp increase and sharp decrease in the figure. Here the sharp decrease is mainly because the arrival of new users, which reduces the instantaneous average value. And the sharp increase is mainly because the agents allocate the RBGs to the user with very high CQI values.

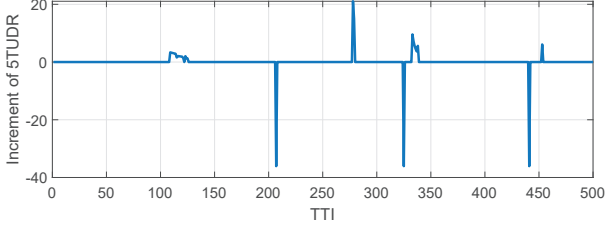


Fig. 4. The increment of 5TUDR between two adjacent TTI in one simulation.

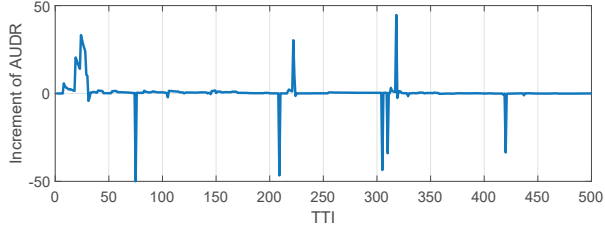


Fig. 5. The increment of AUDR between two adjacent TTI in one simulation.

On the one hand, the scheduling policy is expected to maintain considerable usage of the network resources. To realize this objective, the simplest method is to follow the OP scheduling, which always to allocate the RBGs with high CQI. But this will make the scheduler entirely ignore the inferior users, so that the 5TUDR is greatly decreased. On the other hand, to maximize the 5TUDR, the scheduling can not only focus on the CQI of users, which should pay more attention to other decision basis such as HUDR. But this will also damage the usage of the network resources.

To address this dilemma, we propose the following reward function which both considers the usage and fairness:

$$\mathcal{G}_\sigma(\mathbf{x}) = \prod_{i=1}^n \sin\left(\frac{\pi x_i}{2 \max(\mathbf{x})}\right)^{\frac{1}{\sigma}}, \sigma \in \mathbb{R}^+$$

$$\Delta \Psi_t = (\Delta \psi_t^1, \dots, \Delta \psi_t^{\hat{N}_t}), \Delta \psi_t^i = \psi_t^i - \psi_{t-1}^i \quad (14)$$

$$r_t = h\left(\sum_{i=1}^{N_t} \psi_t^i - \sum_{i=1}^{N_{t-1}} \psi_{t-1}^i\right) - \exp\{-\mathcal{G}_\sigma(\Delta \Psi_t)\}$$

where $\mathcal{G}_\sigma(\cdot) \in [0, 1]$ is the G's fairness index [24], $h(x) = \frac{1}{1+e^{-x}}$ is the sigmoid function, N_t is the number of total

arrived users in the cell, \hat{N}_t is the number of active users in the cell, and $\psi_t^i = 0$. And the reward function of Eq. 14 is designed based on the following insights:

- This reward function conditions on the sum user data rate, which has nothing to do with the time-varying number of total arrived users.
- To maintain the usage of the network resources, the scheduling policy is required to maximize the increment sum user data rate. This encourage the agents to allocate RBGs to the users with higher CQI.
- The G's fairness index is introduced as the punishment item, which conditions on the increment sequence of the individual user data rate. The gain of the sum user data rate can be realized through two possible solutions. One is to only allocate the RBGs to the superior users, which brings tremendous gain in throughput. The other one is to let more users make contribution, which brings smaller gain in throughput. If the agents follow the first method, the agents will be punished. Through the fairness index, the agents will be forced to allocate RBGs more evenly, so as to promote the 5TUDR.

So far all the elements of the stochastic game are obtained. For such game problem, the Nash Equilibrium (NE) is always used to describe the solution [16]. In the NE, each action of a agent is the best response to other agents. But the NE is always difficult to realize in many scenarios. To find the expected scheduling policy in this stochastic game, an learning algorithm based on Multi-Agent Reinforcement Learning (MARL) is proposed in the next section.

IV. MARL-BASED ALGORITHM

The MARL is built to develop and analyzing learning rules and algorithms which can discover effective strategies in multi-agent environments. With powerful self-exploration ability, the MARL is making increasing difference in the construction of AI systems. In this section, we first give some basic elements of the MARL based on the defined stochastic game. Then a QMIX learning algorithm is introduced to maximize the expected long-term return defined in Eq. 13. Finally, the detailed algorithm of MARL for RBG allocation is summarized.

A. MARL Background

The MARL learns from the interactions with the environment and updates its policy to maximize the long-term return. To evaluate the policy, the state-value function and action-value function are introduced to characterize the expected return:

$$V^\pi(\mathbf{s}) = \mathbb{E}\left[\sum_{t=0}^{+\infty} \gamma^t r_t \mid \pi, \mathbf{s}_0 = \mathbf{s}\right]$$

$$Q^\pi(\mathbf{s}, \mathbf{u}) = \mathbb{E}\left[\sum_{t=0}^{\infty} \gamma^t r_t \mid \pi, \mathbf{s}_0 = \mathbf{s}, \mathbf{u}_0 = \mathbf{u}\right] \quad (15)$$

The $V^\pi(\mathbf{s})$ represents the expected return if the agents if the agents continue executing the joint-policy after the global state

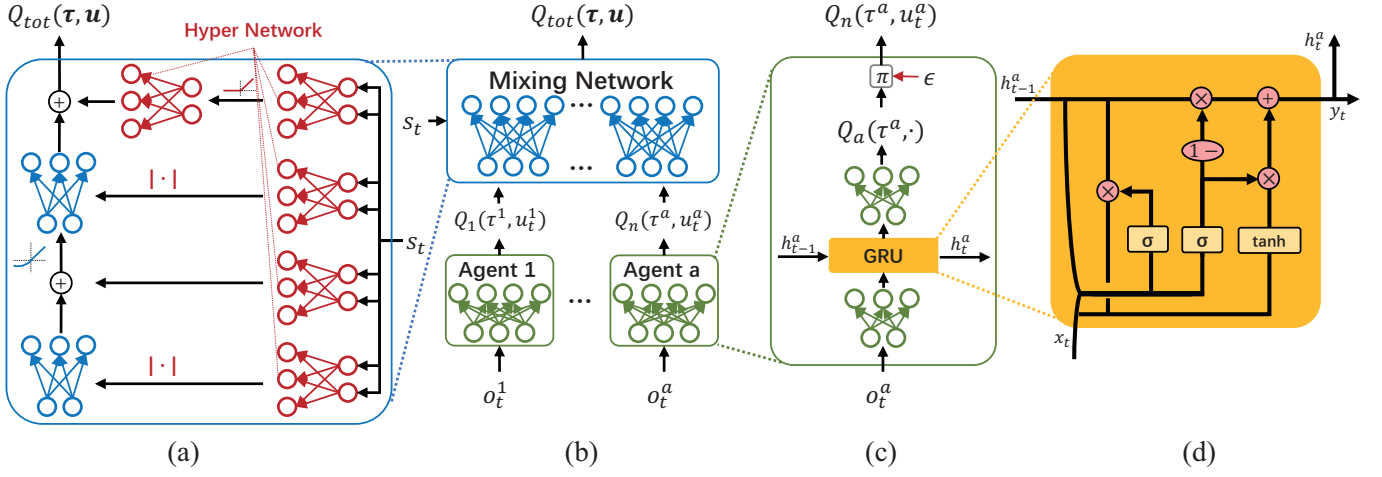


Fig. 6. (a) Mixing network structure. In red are the hypernetworks that produce the weights and biases for mixing network layers shown in blue. (b) The overall QMIX architecture. (c) Agent network structure. (d) The GRU structure, where h is the hidden information used for recursion [25].

s. Similarly, the $Q^\pi(s, \mathbf{u})$ represents the expected return if the agents executing the joint-policy π after taking joint-action \mathbf{u} at the global state s . Based on the action-value function, the value-based RL algorithms choose the action at each step following [10]:

$$\mathbf{u} = \arg \max_{\mathbf{u}} \{Q^\pi(s, \mathbf{u})\} \quad (16)$$

Moreover, the Bellman Optimal Theorem indicates that the optimal policy π^* satisfies:

$$Q^{\pi^*}(s, \mathbf{u}) = Q^*(s, \mathbf{u}) := \sup_{\pi \in \Pi} \{Q^\pi(s, \mathbf{u})\} \quad (17)$$

Therefore the optimal policy π^* can be obtained if the action-value function is maximized. To find such a policy, the iteration method is adopted to carry on the action-value function iteration, which is the well-known Q-learning algorithm [26]. To conduct the iteration, the Bellman Equation Eq. 18 is introduced which describes the relationship between the action-value of a state-action pair and the action-value of the successor state-action pair [27].

$$Q^\pi(s, \mathbf{u}) = \mathbb{E}[r + \gamma Q^\pi(s', \mathbf{u}') | \pi] \quad (18)$$

And the $Q^*(s, \mathbf{u})$ holds the Bellman Optimality Equation:

$$Q^*(s, \mathbf{u}) = \mathbb{E} \left[r + \gamma \max_{\mathbf{u}' \in \mathcal{U}} \{Q^*(s', \mathbf{u}')\} \right] \quad (19)$$

Considering the high dimensional state space, it is inevitable to use function approximation as the representation of action values. Let $Q_\theta^\pi(s, \mathbf{u})$ denote the action-value function parametrized by a DNN with parameters θ . The optimization objective is transformed to find θ that holds $Q_\theta^\pi(s, \mathbf{u}) \approx Q^*(s, \mathbf{u})$. And the optimal parameters θ can be approached by minimizing the following temporal difference error [28]:

$$\mathcal{L}(\theta) = \left[r + \gamma \max_{\mathbf{u}'} \{Q_\theta^\pi(s', \mathbf{u}')\} - Q_\theta^\pi(s, \mathbf{u}) \right]^2 \quad (20)$$

B. QMIX Based RBG allocation

The partially observable setting let each agent maintain an observation history $\tau^a \in \mathcal{T}$. For the environment, there is a joint action-observation history $\tau \in \mathcal{T}^{|\mathcal{A}|}$. Then the action-value function is rewritten as $Q_\theta^\pi(\tau, \mathbf{u})$. It is difficult to straightforwardly learn the optimal action-value function due to the exponential joint-action space. Moreover, the $Q_\theta^\pi(\tau, \mathbf{u})$ can not be used to apply decentralized control. In order to address this problem, the QMIX is introduced to learn the joint-action value function via value decomposition. For convenience, we refer Q_{tot} to the $Q_\theta^\pi(\tau, \mathbf{u})$ in the following sections.

The QMIX is a model-free, value-based, off-policy, decentralized execution and centralized training algorithm towards cooperative task, which takes DNN function approximator to estimate the action-value function [29]. QMIX allows each agent a maintain an individual action-value function $Q_a(\tau^a, u^a)$, which conditions on action-observation history τ^a and local action u^a . Thus the decentralized execution is tractable based on the individual action-value functions. For centralized training, the QMIX leverages a mixing network to calculate the centralized action-value function Q_{tot} . What's more, the QMIX ensures that the global argmax operation applied on the centralized Q_{tot} generates the same result as a set of argmax operation applied on each Q_a :

$$\arg \max_{\mathbf{u}} \{Q_{tot}\} = \begin{pmatrix} \arg \max_{u^1} \{Q_1(\tau^1, u^1)\} \\ \vdots \\ \arg \max_{u^n} \{Q_n(\tau^n, u^n)\} \end{pmatrix} \quad (21)$$

Mathematically, this imposes a monotonicity constraint on the relationship between Q_{tot} and each Q_a :

$$\frac{\partial Q_{tot}}{\partial Q_a} \geq 0, \forall a. \quad (22)$$

Fig. 6 illustrates the framework of QMIX. At each step, each agent a accepts a local observation o^a and generates $|\mathcal{U}|$

action values. Then the action is chosen which accords with the ϵ -greedy principle [30]:

$$\pi^a(u^a|o^a) = \begin{cases} 1 - \epsilon + \frac{\epsilon}{|\mathcal{U}|}, u^a = \arg \max_{u^a} \{Q_a(\tau^a, u^a)\} \\ \frac{\epsilon}{|\mathcal{U}|}, u^a \neq \arg \max_{u^a} \{Q_a(\tau^a, u^a)\} \end{cases} \quad (23)$$

This policy implies that the agent will randomly select an action from the action space with a probability of ϵ , or follow the action with maximum action-value with a probability of $1 - \epsilon$. This policy allows the agents to make sufficient exploration, because it increases the probability of covering all the possible state-action pairs when apply training.

After the individual action-value of all the agents are generated, it is sent to the mixing network to generate the centralized action-value Q_{tot} . The mixing network consists two parts, the backbone and hyper-networks. As the Q_{tot} conditions on the global state \mathbf{s} , the mixing network uses the hyper-network to generate weights and biases for its backbone. Let \mathcal{H}_η and \mathcal{M}_β denote the hyper-network and the mixing network parameterized by parameters η and β respectively. At each step t , the hyper-network accepts the global state \mathbf{s} and generates weights and biases:

$$\beta_t \leftarrow \mathcal{H}_\eta(\mathbf{s}_t) \quad (24)$$

Moreover, all the generated weights are positive to hold the Eq. 22. Considering the mixing network in Fig. 6, let W_1, W_2, B_1, B_2 denote the generated weights and biases from the hypernetworks, $\mathbf{Q} = \{Q_1, \dots, Q_n\}$ being the input vector and $g(x) = \begin{cases} \alpha(e^x - 1), x < 0, \alpha > 0 \\ x, x \geq 0 \end{cases}$ being the ELU activation function. Thus the Q_{tot} can be written as:

$$\begin{aligned} Q_{tot} &= W_2 g(W_1 \mathbf{Q} + B_1) + B_2 \\ &= W_2 g(Y_1) + B_2 \end{aligned} \quad (25)$$

Then,

$$\begin{aligned} \frac{\partial Q_{tot}}{\partial \mathbf{Q}} &= \frac{\partial Q_{tot}}{\partial g(Y_1)} \cdot \frac{\partial g(Y_1)}{\partial Y_1} \cdot \frac{\partial Y_1}{\partial \mathbf{Q}} \\ &= W_2 \cdot g'(W_1 \mathbf{Q} + B_1) \cdot W_1 \end{aligned} \quad (26)$$

Since

$$g'(x) = \begin{cases} \alpha e^x, x < 0, \alpha > 0 \\ 1, x \geq 0 \end{cases} \quad (27)$$

And W_1, W_2 is non-negative, thus:

$$\frac{\partial Q_{tot}}{\partial Q_a} \geq 0, \forall a. \quad (28)$$

Through the hyper-network, the global state is integrated to build the centralized action-value function. Finally, the QMIX is trained by minimizing the following loss function:

$$\mathcal{L}(\boldsymbol{\theta}, \eta) = [r + \gamma \max_{\mathbf{u}'} Q_{tot}(\boldsymbol{\tau}', \mathbf{u}', \mathbf{s}') - Q_{tot}(\boldsymbol{\tau}, \mathbf{u}, \mathbf{s})]^2 \quad (29)$$

where the $\boldsymbol{\theta}$ is the parameters set of the agents. Eq. 29 is similar to Eq. 20, along with update operations. Finally, the QMIX for searching the scheduling policy for the RBG allocation is summarized in Algo. 1

Algorithm 1 QMIX for RBG Allocation

- 1: Initialize $|K|$ agent networks $Q_{\theta_1} : \mathcal{T} \rightarrow \mathbb{R}^{|\mathcal{U}|}, \dots, Q_{\theta_{|K|}} : \mathcal{T} \rightarrow \mathbb{R}^{|\mathcal{U}|}$ with parameters $\boldsymbol{\theta} = (\theta_1, \dots, \theta_{|K|})$.
 - 2: Initialize hyper-network \mathcal{H}_η and mixing network \mathcal{M}_{β_0} with parameters η and β_0 .
 - 3: Set a replay buffer \mathcal{B} , learning rate λ , discount factor γ and ϵ .
 - 4: **for** Epoch = 1, ..., E **do**
 - 5: Initialize the base station with a set of K RBGs and randomly generate \hat{N}_1 initial users.
 - 6: Each agent receives the initial local observation \mathbf{o}_1^a
 - 7: **for** $t = 1, \dots, T$ **do**
 - 8: New users arrive at the cell according to the Poisson distribution.
 - 9: Each agent a makes local action u_t^a following the ϵ -greedy policy and observe a new local state \mathbf{o}_{t+1}^a .
 - 10: Execute the joint-action \mathbf{u}_t and observe the global reward r_t , then observe a new global state \mathbf{s}_{t+1} .
 - 11: Store the following transition in \mathcal{B} :
$$(\mathbf{s}_t, r_t, \mathbf{s}_{t+1}, \mathbf{o}_t^a, \mathbf{o}_{t+1}^a, \mathbf{u}_t^a, \mathbf{h}_{t-1}^a, \mathbf{h}_t^a)$$
 - 12: Sample a random minibatch of b transitions from \mathcal{B} :
$$(\mathbf{s}_i, r_i, \mathbf{s}_{i+1}, \mathbf{o}_i^a, \mathbf{o}_{i+1}^a, \mathbf{u}_i^a, \mathbf{h}_{i-1}^a, \mathbf{h}_i^a)$$
 - 13: Get $|K|$ individual Q values:
$$\begin{aligned} \mathbf{Q}_{\theta_a} &= (Q_{\theta_1}(\tau^1, u_i^1), \dots, Q_{\theta_{|K|}}(\tau^{|K|}, u_i^{|K|})) \\ \mathbf{Q}'_{\theta_a} &= (Q_{\theta_1}(\tau^{1'}, u_{i+1}^1), \dots, Q_{\theta_{|K|}}(\tau^{|K|'}, u_{i+1}^{|K|})) \end{aligned}$$
 - 14: Calculate weights for mixing network, then get Q_{tot} and Q'_{tot} :
$$\begin{aligned} \beta_i &\leftarrow \mathcal{H}_\eta(\mathbf{s}_i), \beta_{i+1} \leftarrow \mathcal{H}_\eta(\mathbf{s}_{i+1}) \\ Q_{tot}(\boldsymbol{\tau}, \mathbf{u}_i, \mathbf{s}_i; \beta_i) &\leftarrow \mathcal{M}_{\beta_i}(\mathbf{Q}_{\theta_a}) \\ Q'_{tot}(\boldsymbol{\tau}', \mathbf{u}_{i+1}, \mathbf{s}_{i+1}; \beta_{i+1}) &\leftarrow \mathcal{M}_{\beta_{i+1}}(\mathbf{Q}'_{\theta_a}) \end{aligned}$$
 - 15: Set $y_i = r_i + \gamma \max_{\mathbf{u}_{i+1}} \{Q'_{tot}(\boldsymbol{\tau}', \mathbf{u}_{i+1}, \mathbf{s}_{i+1}; \beta_{i+1})\}$
 - 16: Update all the agent networks and hyper-network by minimizing the following loss:
$$\mathcal{L}(\boldsymbol{\theta}, \eta) = \sum_{i=1}^b \left[(y_i - Q_{tot}(\boldsymbol{\tau}, \mathbf{u}_i, \mathbf{s}_i; \beta_i))^2 \right]$$
 - 17: **end for**
 - 18: **end for**
-

V. SIMULATION RESULTS AND NUMERICAL ANALYSIS

So far the problem modeling is accomplished and the solution is obtained. In this section, we demonstrate the simulation results and the corresponding numerical analysis. All the simulations are conducted based on the network defined in Section II, which follows the mechanisms in Appendix A. The Table III illustrates the parameters of the base station.

TABLE III
PARAMETERS FOR THE BASE STATION.

| Parameters | Values |
|----------------------------------|-------------|
| Transmit power for each RB | 18 dBm |
| Number of RB for each RBG | 3 |
| Number of RBGs | 3 |
| Frequency bandwidth for each RBG | 10MHz |
| Noise power density | -174 dBm/Hz |
| Minimum MCS | 1 |
| Maximum MCS | 29 |
| Mximum number of HARQ | 8 |
| Feedback period of HARQ | 8 |
| Initial RB CQI value | 4 |

We deploy 3 RBGs in the base station to testify the proposed algorithm. Here each RBG is composed of three RBs, whose transmit power is 18dBm. For transmission, each user owes at most HARQ processes, which will be informed the ACK/NACK message in seven TTIs.

A. Model Training

The agents is trained following the parameters listed in Table IV. Here one epoch represents one allocation process whose duration is 1000TTIs. For each epoch, the base station will continue to accept data requests and the agents will make allocation until the duration is over. This produces much experiences which are composed of the state-action pairs and the corresponding rewards. Then the agents will select a minibatch of experiences to update its parameters. The batches and the batch size are set as 10 and 256 respectively, where the batch size means the amount of the experiences in each minibatch.

TABLE IV
PARAMETERS FOR TRAINING.

| Parameters | Values |
|---------------------------------|----------|
| Epochs | 100 |
| Duration of one epoch | 1000TTIs |
| Learning rate | 1e-3 |
| Learning rate decay | 1e-7 |
| Batches | 10 |
| Batch size | 256 |
| Replayer capacity | 2000 |
| ϵ | 1e-2 |
| Initial number of users | 5 |
| Average of Possion distribution | 1e-2 |

As can be seen in the Fig. 7, the episode reward of each epoch increasing stably with the progress of the training.

B. Performance Comparison

To demonstrate the performance of the proposed scheduler, we compare it with two traditional schedulers, which are the PF scheduling and the RRF scheduling. We define these scheduling algorithms in the Appendix B.

In this paper, we aim to maximize the 5TUDR of the network. For the PF scheduling, the scheduler is considered as the most fairness-oriented when $\alpha_1 = 0, \alpha_2 = 1$ [6]. Here the PF scheduling only takes the historical user data rate to

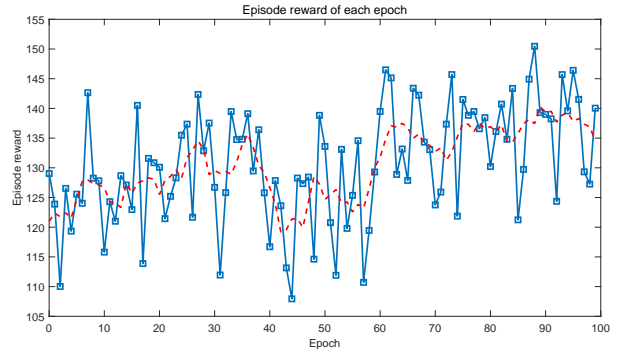


Fig. 7. Episode reward for each epoch

calculate the allocation priorities. But the realistic situation might be different in the bursty traffic, because the scheduler may not attain the whole capacity of the network.

To investigate the highest 5TUDR that the PF scheduling may achieve, we attempt to measure experience-based value through large amount of simulations. We take the RRF scheduling and the OP scheduling as the baseline, then perform the simulations using PF scheduling with different coefficients (listed in Table V).

TABLE V
LIST OF SCHEDULERS.

| Schedulers | Remarks |
|----------------|--|
| RRF scheduling | N/A |
| PF scheduling | $\alpha_1 = 0, 0.02, \dots, 0.98, 1, \alpha_2 = 1$ |
| OP scheduling | N/A |

As can be seen in Fig. 8, the PF scheduling achieves higher 5TUDR with the increase of α_1 , and it finally stabilized at about $\alpha_1 = 0.5$. When the α_1 is nonzero, the PF scheduling starts to consider the instantaneous estimated user data rate. The advantage users with better channel will take higher allocation priorities and produce more throughput, which not only promotes the usage of the network resources but also contributes to the 5TUDR. Therefore, the following evaluations are performed with four schedulers, which are MARL scheduling, PF1 scheduling ($\alpha_1 = 0, \alpha_2 = 1$), PF2 scheduling ($\alpha_1 = 0.5, \alpha_2 = 1$) and RRF scheduling respectively.

Similar to the model training, 100 random simulations are performed to verify the performance of the four schedulers, and the AUDR and 5TUDR are calculated respectively. Fig. 9 and Fig. 10 illustrate the corresponding cumulative distribution function (CDF) of the performance difference. The CDF manifests that the MARL scheduler achieving a 83.20Bits/TTI, -29.84Bits/TTI and 147Bits/TTI AUDR gain in contrast with PF1, PF2 and RRF respectively. Moreover, the MARL scheduler achieving a 54.70Bit/TTI, 39.42Bits/TTI and 46.96Bits/TTI 5TUDR gain compared with PF1, PF2 and RRF respectively. Therefore, the proposed MARL-based scheduler successfully realizes the promotion of the 5TUDR while maintaining the considerable AUDR.

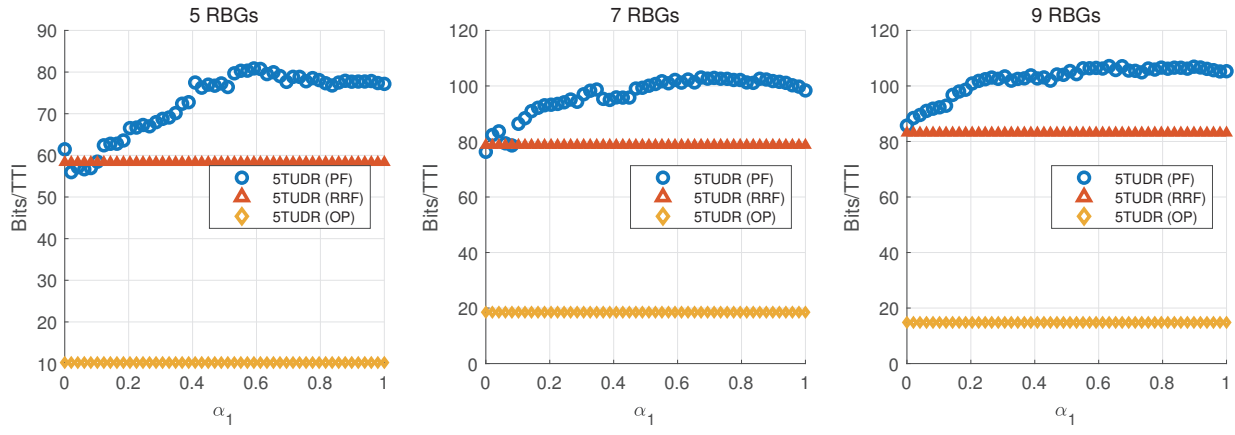


Fig. 8. Average 5TUDR of different schedulers in 1000 random simulations.

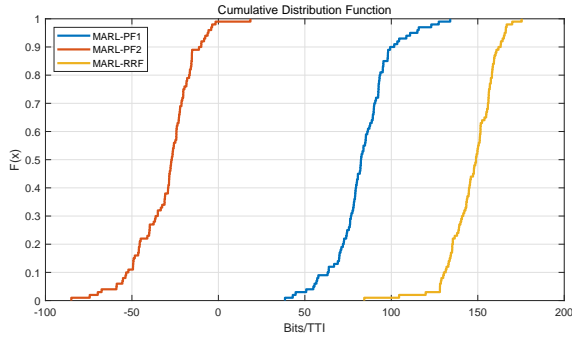


Fig. 9. CDF of performance difference in AUDR.

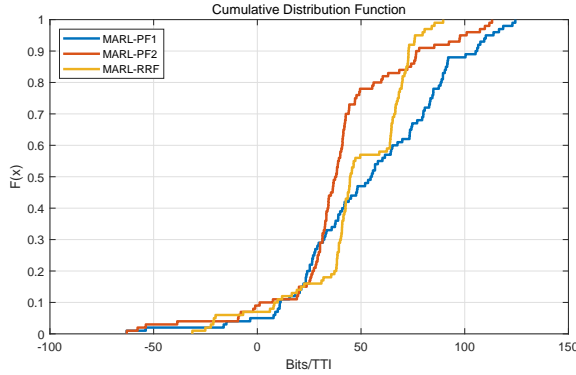


Fig. 10. CDF of performance difference in 5TUDR.

C. Policy Analysis

Different from the traditional schedulers which have explicit formulations, the learned MARL-based scheduler is black box with a set of the network parameters. So it is difficult to straightforwardly analyze its scheduling policy. In this section, we attempt to demonstrate the different scheduling preference between the four schedulers by analyzing the allocation log. Considering the specific bursty traffic that there is only finite users in the cell and no new users, 5 users and 3 RBGs are

deployed in the cell to conduct interactions for 500TTIs.

1) *More Transmission Time and Less Residence Time*: We first investigate the total transmission time and total residence time of the five users. The total transmission time implies that how many times the users get RBGs. For instance, if the three RBGs are allocated to three users respectively, the transmission time will be added by 3. On the contrary, the residence time implies that how many times the users need to finish its requests including the waiting time. As can be seen in the Fig. 11, the MARL-based scheduler significantly decreases the total residence time of the users. This indicates that the requests of the users can be satisfied more quickly under the allocation of the MARL-based scheduler. Meanwhile, the total transmission time of the users is significantly increased, which means the users take less waiting time. So the users can finish its data requests as quick as possible, which produces higher AUDR.

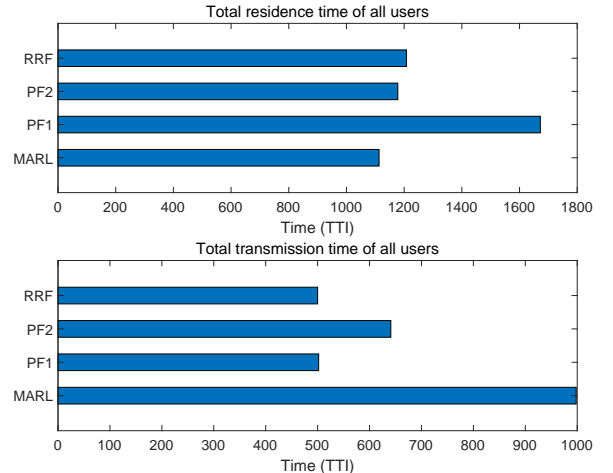


Fig. 11. Total residence time and total transmission time.

2) *Distributional Allocation*: Compared with other schedulers, the MARL-based scheduler creates the highest total transmission time. This indicates the MARL-based scheduler

prefers to make distributional allocation rather than centralized allocation. The Table VI and Table VII illustrates the allocation result in TTI=1 and TTI=100. Here the "T" and "F" represent the allocation result of the RBGs, "N/A" means the user has finished its transmission. For instance, the "T" of 8th row means the RBG#1 is allocated to the UE#4 in Table VI. In this TTI, the PF2 and RRF allocate all the RBGs to the same user, while the MARL scheduler and PF2 scheduler distribute the RBGs to different users. Furthermore, we calculate the time that the users get at least one RBG, and the statistical data is shown in the Fig. 12. Here the "one" means that the scheduler allocates one RBG to a single user in TTI t . Similarly, "two" means that the scheduler allocates two RBGs to a single user in TTI t .

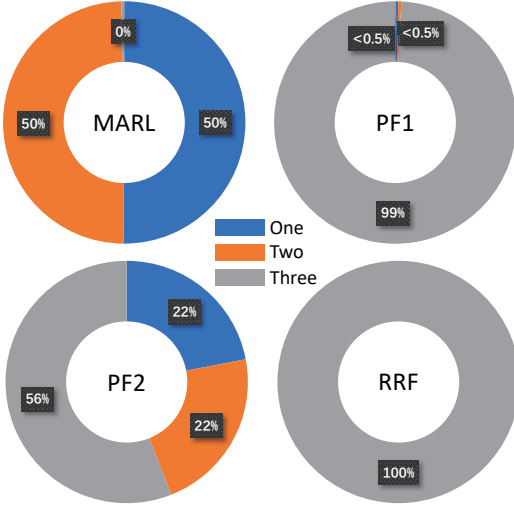


Fig. 12. Total transmission time with different number of RBGs.

As can be seen in the Fig. 12, the PF1 scheduler and the RRF scheduler almost allocate all the RBGs to single user during the whole communication process. However, the MARL scheduler and the PF2 scheduler choose to distribute the RBGs to different users. In each TTI, the users are provided more opportunity to get RBGs under the scheduling of the MARL scheduler and the PF2 scheduler, which realizes higher allocation fairness. The allocation of the MARL scheduler is more distributional than the MARL scheduler, because the MARL scheduler almost never allow the users to monopolize the RBGs, which produces higher total transmission time and allocation fairness.

3) *Scheduling Preference*: Finally, we attempt to find out the scheduling preference of the MARL scheduler. The policy of the MARL scheduler is a series of DNN parameters, which is intractable to demonstrate or summarize. But we can still infer the scheduling tendency through the data analysis of the allocation log. In the simulation of the Table VI and Table VII, the UE#1 and UE#2 take bigger buffer size than the other three users. In TTI=100, the MARL scheduler accomplishes more user requests than the other schedulers. Moreover, the left users are the three users who take smaller buffer size.

TABLE VI
ALLOCATION EXAMPLE 1 (TTI=1)

| Attr. | UE#1 | UE#2 | UE#3 | UE#4 | UE#5 | |
|--------|-------|-------|-------|------|-------|---|
| RSRP | -99 | -90 | -96 | -88 | -70 | |
| Buffer | 94768 | 96288 | 15528 | 4400 | 36400 | |
| HUDR | 0.0 | 0.0 | 0.0 | 0.0 | 0.0 | |
| CQI#1 | 4 | 4 | 4 | 4 | 4 | |
| CQI#2 | 4 | 4 | 4 | 4 | 4 | |
| CQI#3 | 4 | 4 | 4 | 4 | 4 | |
| MARL | RBG#1 | F | F | F | T | F |
| | RBG#2 | T | F | F | F | F |
| | RBG#3 | F | F | F | T | F |
| PF1 | RBG#1 | T | F | F | F | F |
| | RBG#2 | T | F | F | F | F |
| | RBG#3 | T | F | F | F | F |
| PF2 | RBG#1 | T | F | F | F | F |
| | RBG#2 | T | F | F | F | F |
| | RBG#3 | T | F | F | F | F |
| RRF | RBG#1 | T | F | F | F | F |
| | RBG#2 | T | F | F | F | F |
| | RBG#3 | T | F | F | F | F |

TABLE VII
ALLOCATION EXAMPLE 2 (TTI=100)

| Attr. | UE#1 | UE#2 | UE#3 | UE#4 | UE#5 | |
|--------|-------|-------|------|------|------|---|
| RSRP | -99 | -90 | N/A | N/A | N/A | |
| Buffer | 86119 | 89886 | N/A | N/A | N/A | |
| HUDR | 72.1 | 42.9 | N/A | N/A | N/A | |
| CQI#1 | 7 | 9 | N/A | N/A | N/A | |
| CQI#2 | 7 | 9 | N/A | N/A | N/A | |
| CQI#3 | 3 | 14 | N/A | N/A | N/A | |
| MARL | RBG#1 | T | F | F | F | F |
| | RBG#2 | T | F | F | F | F |
| | RBG#3 | F | T | F | F | F |
| PF1 | RBG#1 | T | F | F | F | F |
| | RBG#2 | T | F | F | F | F |
| | RBG#3 | T | F | F | F | F |
| PF2 | RBG#1 | T | F | F | F | F |
| | RBG#2 | T | F | F | F | F |
| | RBG#3 | F | T | F | F | F |
| RRF | RBG#1 | T | F | F | F | F |
| | RBG#2 | T | F | F | F | F |
| | RBG#3 | T | F | F | F | F |

Therefore, it is reasonable to assume that the MARL scheduler prefers to allocate the users with less buffer first. To test the assumption, we first investigate the number of active users in each TTI under the allocation of different schedulers. The Fig. 13 shows that the MARL scheduler takes less time but satisfies more requests. Based on the Fig. 13, we further investigate the scheduled time of the three users from TTI=1 to TTI=83. For instance, if the user is allocated with 2 RBGs, then the scheduled time will be calculated as 2. As can be seen the Fig. 14, it is obvious that the MARL scheduler spends more time on these users. By accelerating the transmission of the small users, the MARL scheduler promotes the UDR of the small users, which finally contributes to the AUDR.

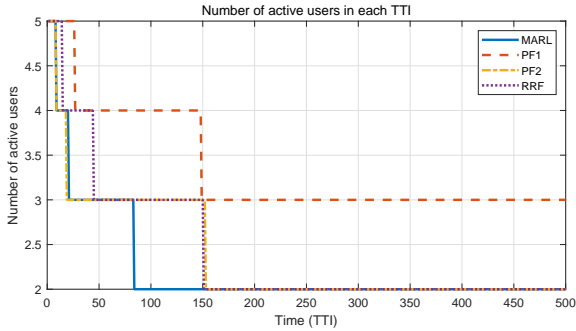


Fig. 13. Number of active users in each TTI.

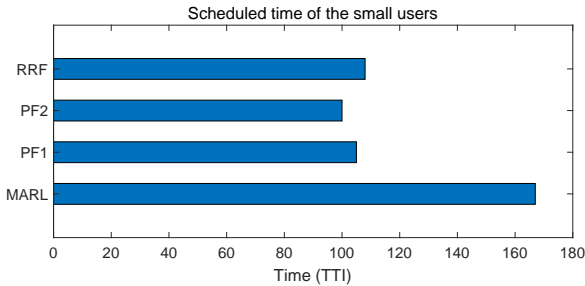


Fig. 14. Scheduled time of the small users.

As for other features, we calculate the spearman correlation coefficient matrix, which is illustrated in Fig. 15. For instance, the correlation coefficient between the allocation result of the RBG#1 and buffer is 0.6308, which means great correlation. This also shows that there is no strong correlation between the allocation result and the other features. So we do not make further elaboration.

Finally, the scheduling policy of the MARL scheduler can be summarized as follows:

- A distributional policy that prefers to distributes the RBGs to different users to promote the allocation fairness. Under the allocation of the MARL scheduler, the users have more opportunity to get resources rather than just waiting. Such operation guarantees that all the users can contribute to the transmission rate, so as to promote the 5TUDR. This also proves the proposed reward function indeed controls the learning direction of the agents.

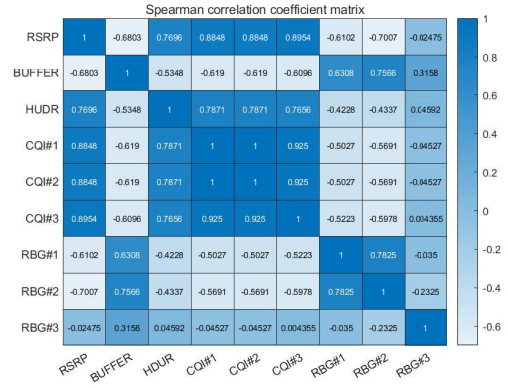


Fig. 15. Spearman correlation coefficient matrix.

- To keep the usage of the system resources, the MARL scheduler tries to satisfy the requests of small users as fast as possible. By reducing the transmission time of the small users, the MARL scheduler achieves considerable UDR gain, which greatly contributes the of the final AUDR.
- The scheduling policy of the MARL scheduler is forward-looking, it can conduct macroscopic and long-term allocation to realize the final objective. Although the MARL scheduler can not be thoroughly understood due to complexity of the DNN, but it still demonstrates the great potential of the MARL in user scheduling.

VI. CONCLUSION

In this work, we investigate the problem scheduling, especially the RBG allocation. To maximize the fairness performance of the communication system, a fairness-oriented scheduler is proposed based on multi-agent reinforcement learning. This scheduler can allocates multiple RBGs to multiple users in the bursty, and achieve the highest 5%-tile user data rate compared with the PF scheduling and the RRF scheduling. Furthermore, we analyze the scheduling policy of the MARL scheduler is fully from diverse perspectives, such as allocation time and so on. There are still much development space about the combination of user scheduling and reinforcement learning, and we will further improve the MARL-based scheduler which can optimize both the fairness and throughput. And we fully believe that the reinforcement learning will be utilized to make more pioneering work in the future.

APPENDIX

A. Network mechanism

1) *Out Loop Link Adaptation*: On the user side, CQI levels represent the received signal-to-noise ratio (SNR) on each resource block (RB), and they are periodically computed and reported. Thus the received instantaneous SNR directly influences the selection of MCS. However, it should be noted that there is a CQI offset reflecting the detection sensitivity per user which is unknown to the BS. Thus, to compensate

for the discrepancy between the chosen MCS and the optimal MCS for different users. An OLLA process is carried out on BS to offset a CQI value q , which is

$$\bar{q} = [q + \alpha], \quad (30)$$

where $[\cdot]$ is the rounding operation and \bar{q} is the offset CQI readily for MCS selection. Besides, α is the adjustment coefficient given by

$$\alpha = \begin{cases} \alpha + s_A, & \mathfrak{A} = 1, \\ \alpha + s_N, & \mathfrak{A} = 0, \end{cases} \quad (31)$$

where \mathfrak{A} is the corresponding ACK/NACK feedback with “1” indicating a successful transmission while “0” a failed transmission, and the update rate $s_A > 0$ and $s_N < 0$ can be customized.

2) *Transmission Block Formation*: Let $\mathcal{F}(q)$ denote the mapping from the CQI \bar{q} to its spectral efficiencies (SE), and \mathcal{I} denote a set of CQI levels measured by a user in terms of a group of RBs. The supportive number of bits that can be loaded to the group of RBs for the user is given by

$$f(\mathcal{I}) = |\mathcal{I}| \cdot \mathcal{F} \left(\left\lfloor \frac{1}{|\mathcal{I}|} \sum_i \{\mathcal{I}\}_i \right\rfloor \right) \quad (32)$$

where $\lfloor \cdot \rfloor$ is the floor function. For instance, the estimated data rate of user n in RBG k can be obtained by $R_{n,k} = f(\mathcal{I}_n(k))$, where $\mathcal{I}_n(k)$ is the set of all RBs in RBG k measured by user n . When multiple RBGs are allocated to the user, they are utilized to convey one transport block (TB) with the same MCS. The size of data loaded to the TB is given by $T_n = f(\mathcal{I}_n)$, where \mathcal{I}_n is the set of all RBs allocated to user n .

3) *Hybrid Automatic Repeat reQuest and Retransmission*: When a TB is packed for a user, the corresponding data will be loaded to a HARQ buffer and cleared out from the data buffer. The BS can arrange at most eight HARQ processes (each with a HARQ buffer) for each user, and will see an ACK/NACK message from the corresponding user in seven TTIs. In the case of ACK, the HARQ process terminates, while in the case of NACK, a retransmission is triggered and the HARQ process is still held. The RBGs initially delegated to the first transmission will conduct the retransmission, thus being unavailable for user scheduling temporarily. The MCS selection and TB size remain the same for the retransmission and the HARQ process will expire at five times of consecutive failure, which literally causes the so-called packet loss.

B. Benchmark schemes

Here gives the definition of PF scheduling and RRF scheduling which adopted in this work.

1) *Proportional Fairness Scheduling (PF)*: In the PF scheduling, any user with a non-empty buffer is a candidate to each RBG, and each RBG independently sort all users according to their PF values. Denote the PF value of user n on RBG k within transmission time interval (TTI) i by $\zeta_{n,k}[i]$, then we have

$$\zeta_{n,k}[i] = \frac{(R_{n,k}[i])^{\alpha_1}}{(\hat{T}_n[i])^{\alpha_2}}, \quad (33)$$

where $\hat{T}_n[i]$ is the user’s moving average throughput which can be expressed as

$$\hat{T}_n[i] = (1 - \chi) \hat{T}_n[i - 1] + \chi T_n[i - 1]. \quad (34)$$

In Eq. (34), χ is the moving average coefficient, and $T_n[i - 1]$ is the actual TB size of user n in TTI $i - 1$. The users with higher PF value hold higher priority to occupy the RBG, and the PF value of a user to different RBGs can be different. Specifically, the PF scheduling can be expressed as

$$P_{PF}^*(k) = \arg \max_n \{\zeta_{n,k}\}, \quad (35)$$

2) *Opportunistic Scheduling (OP)*: As the optimal scheduling in terms of systematic throughput maximization, opportunistic user scheduling is quite straightforward, which can be expressed as

$$P_{OP}^*(k) = \arg \max_n \{R_{n,k}\}. \quad (36)$$

It means each RBG selects the user suggesting the highest estimated data rate, which also implies the optimal scheduling in achieving the highest AUDR in the full buffer traffic but not necessarily in the bursty traffic.

3) *Round Robin Fashion Scheduling (RRF)*: A user scheduling allocates all RBGs to each one user in turns regardless of their status. New users are appended to the end of the queue.

REFERENCES

- [1] W. Saad, M. Bennis, and M. Chen, “A vision of 6g wireless systems: Applications, trends, technologies, and open research problems,” *IEEE Network*, vol. 34, no. 3, pp. 134–142, 2020.
- [2] S. Dang, O. Amin, B. Shihada, and M.-S. Alouini, “From a human-centric perspective: What might 6g be?,” *arXiv preprint arXiv:1906.00741*, 2019.
- [3] K. B. Letaief, W. Chen, Y. Shi, J. Zhang, and Y. A. Zhang, “The roadmap to 6g: Ai empowered wireless networks,” *IEEE Communications Magazine*, vol. 57, no. 8, pp. 84–90, 2019.
- [4] X. Liu, E. K. P. Chong, and N. B. Shroff, “Opportunistic transmission scheduling with resource-sharing constraints in wireless networks,” *IEEE Journal on Selected Areas in Communications*, vol. 19, no. 10, pp. 2053–2064, 2001.
- [5] E. L. Hahne, “Round-robin scheduling for max-min fairness in data networks,” *IEEE Journal on Selected Areas in communications*, vol. 9, no. 7, pp. 1024–1039, 1991.
- [6] D. Tse and P. Viswanath, *Fundamentals of wireless communication*. Cambridge university press, 2005.
- [7] D. Tse, “Multiuser diversity in wireless networks,” in *Wireless Communications Seminar, Stanford University*, 2001.
- [8] G. Zhu, D. Liu, Y. Du, C. You, J. Zhang, and K. Huang, “Toward an intelligent edge: wireless communication meets machine learning,” *IEEE Communications Magazine*, vol. 58, no. 1, pp. 19–25, 2020.
- [9] Q. Cao, S. Zeng, M.-O. Pun, and Y. Chen, “Network-level system performance prediction using deep neural networks with cross-layer information,” in *ICC 2020-2020 IEEE International Conference on Communications (ICC)*, pp. 1–6, IEEE, 2020.
- [10] R. S. Sutton and A. G. Barto, *Reinforcement learning: An introduction*. MIT press, 2018.
- [11] I.-S. Comşa, S. Zhang, M. Aydin, P. Kuonen, R. Trestian, and G. Ghinea, “A comparison of reinforcement learning algorithms in fairness-oriented ofdma schedulers,” *Information*, vol. 10, no. 10, p. 315, 2019.
- [12] I.-S. Comşa, S. Zhang, M. E. Aydin, P. Kuonen, Y. Lu, R. Trestian, and G. Ghinea, “Towards 5g: A reinforcement learning-based scheduling solution for data traffic management,” *IEEE Transactions on Network and Service Management*, vol. 15, no. 4, pp. 1661–1675, 2018.

- [13] C. Xu, J. Wang, T. Yu, C. Kong, Y. Huangfu, R. Li, Y. Ge, and J. Wang, "Buffer-aware wireless scheduling based on deep reinforcement learning," in *2020 IEEE Wireless Communications and Networking Conference (WCNC)*, pp. 1–6, IEEE, 2020.
- [14] Y. Hua, R. Li, Z. Zhao, X. Chen, and H. Zhang, "Gan-powered deep distributional reinforcement learning for resource management in network slicing," *IEEE Journal on Selected Areas in Communications*, vol. 38, no. 2, pp. 334–349, 2019.
- [15] L. Buşoniu, R. Babuška, and B. De Schutter, "Multi-agent reinforcement learning: An overview," in *Innovations in multi-agent systems and applications-1*, pp. 183–221, Springer, 2010.
- [16] R. B. Myerson, *Game theory*. Harvard university press, 2013.
- [17] O. Vinyals, I. Babuschkin, W. M. Czarnecki, M. Mathieu, A. Dudzik, J. Chung, D. H. Choi, R. Powell, T. Ewalds, P. Georgiev, *et al.*, "Grandmaster level in starcraft ii using multi-agent reinforcement learning," *Nature*, vol. 575, no. 7782, pp. 350–354, 2019.
- [18] Shapley and S. L., "Stochastic games," *Proceedings of the National Academy of Sciences*, vol. 39, no. 10, pp. 1095–1100, 1953.
- [19] G. E. Monahan, "State of the art—a survey of partially observable markov decision processes: theory, models, and algorithms," *Management science*, vol. 28, no. 1, pp. 1–16, 1982.
- [20] J. D. Williams and S. Young, "Partially observable markov decision processes for spoken dialog systems," *Computer Speech & Language*, vol. 21, no. 2, pp. 393–422, 2007.
- [21] K. Hornik, M. Stinchcombe, H. White, *et al.*, "Multilayer feedforward networks are universal approximators.," *Neural networks*, vol. 2, no. 5, pp. 359–366, 1989.
- [22] I. Goodfellow, Y. Bengio, A. Courville, and Y. Bengio, *Deep learning*, vol. 1. MIT press Cambridge, 2016.
- [23] D. Michie, D. J. Spiegelhalter, C. Taylor, *et al.*, "Machine learning," *Neural and Statistical Classification*, vol. 13, no. 1994, pp. 1–298, 1994.
- [24] R. K. Jain, D.-M. W. Chiu, W. R. Hawe, *et al.*, "A quantitative measure of fairness and discrimination," *Eastern Research Laboratory, Digital Equipment Corporation, Hudson, MA*, 1984.
- [25] K. Cho, B. Van Merriënboer, D. Bahdanau, and Y. Bengio, "On the properties of neural machine translation: Encoder-decoder approaches," *arXiv preprint arXiv:1409.1259*, 2014.
- [26] C. J. Watkins and P. Dayan, "Q-learning," *Machine learning*, vol. 8, no. 3-4, pp. 279–292, 1992.
- [27] R. Bellman, "Dynamic programming," *Science*, vol. 153, no. 3731, pp. 34–37, 1966.
- [28] V. Mnih, K. Kavukcuoglu, D. Silver, A. Graves, I. Antonoglou, D. Wierstra, and M. Riedmiller, "Playing atari with deep reinforcement learning," *arXiv preprint arXiv:1312.5602*, 2013.
- [29] P. Sunehag, G. Lever, A. Gruslys, W. M. Czarnecki, V. F. Zambaldi, M. Jaderberg, M. Lanctot, N. Sonnerat, J. Z. Leibo, K. Tuyls, *et al.*, "Value-decomposition networks for cooperative multi-agent learning based on team reward.," in *AAMAS*, pp. 2085–2087, 2018.
- [30] M. Wunder, M. L. Littman, and M. Babes, "Classes of multiagent q-learning dynamics with epsilon-greedy exploration," in *Proceedings of the 27th International Conference on Machine Learning (ICML-10)*, pp. 1167–1174, Citeseer, 2010.